

Targeted Degradation of Oncogenic KRAS^{G12C} by VHL-Recruiting PROTACs

Michael J. Bond,[¶] Ling Chu,[¶] Dhanusha A. Nalawansa, Ke Li, and Craig M. Crews*



Cite This: *ACS Cent. Sci.* 2020, 6, 1367–1375



Read Online

ACCESS |



Metrics & More

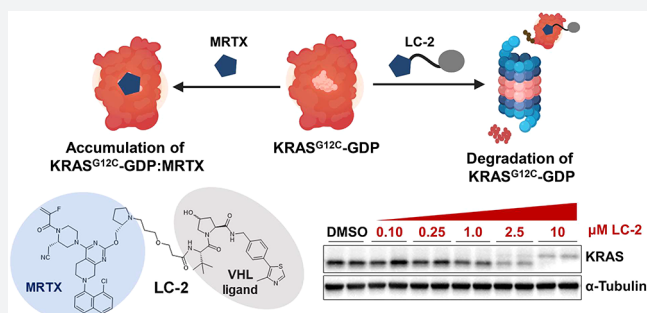


Article Recommendations



Supporting Information

ABSTRACT: KRAS is mutated in ~20% of human cancers and is one of the most sought-after targets for pharmacological modulation, despite having historically been considered “undruggable.” The discovery of potent covalent inhibitors of the KRAS^{G12C} mutant in recent years has sparked a new wave of interest in small molecules targeting KRAS. While these inhibitors have shown promise in the clinic, we wanted to explore PROTAC-mediated degradation as a complementary strategy to modulate mutant KRAS. Herein, we report the development of LC-2, the first PROTAC capable of degrading endogenous KRAS^{G12C}. LC-2 covalently binds KRAS^{G12C} with a MRTX849 warhead and recruits the E3 ligase VHL, inducing rapid and sustained KRAS^{G12C} degradation leading to suppression of MAPK signaling in both homozygous and heterozygous KRAS^{G12C} cell lines. LC-2 demonstrates that PROTAC-mediated degradation is a viable option for attenuating oncogenic KRAS levels and downstream signaling in cancer cells.



INTRODUCTION

The Kirsten rat sarcoma viral oncogene homologue (*KRAS*) gene is one of the most frequently mutated oncogenes in cancer.^{1–3} *KRAS* encodes a small, membrane-bound GTPase that relays signals from receptor tyrosine kinases (RTKs), promoting cell proliferation, cell differentiation, or cell survival.^{4,5} In normal cells, *KRAS* functions as a molecular switch, cycling between an inactive, GDP-bound “off” state and an active, GTP-bound “on” state.^{4,6} This switch is tightly regulated by guanine nucleotide exchange factor (GEF) proteins, which exchange GDP for GTP, and GTPase-activating proteins (GAPs), which enhance the intrinsically slow GTPase activity of *KRAS*.^{7–9} GEF and GAP effector proteins bind at one or both of two shallow binding pockets on *KRAS* termed switch I (residues 30–38) and switch II (residues 59–76), the conformations of which change dramatically between the GDP- and GTP-bound states.^{6,10,11} Somatic *KRAS* mutations attenuate the GAP-mediated enzymatic activity of the protein, resulting in accumulation of GTP-bound, active *KRAS* and hyperactivation of downstream signaling, which leads to uncontrolled cell proliferation.^{1,5} Despite its prevalence in cancer and many years of extensive research efforts, mutant *KRAS* has remained a challenging therapeutic target given the scarcity of traditional druggable pockets on its surface.¹²

The *KRAS p.G12C* mutation is highly prevalent in lung adenocarcinoma (LUAD). *KRAS*^{G12C} mutants make up over 50% of all *KRAS* mutant LUAD tumors (13% of total LUAD tumors).¹ Additionally, 3% of colorectal cancers and 1% of all

other solid tumors express *KRAS*^{G12C}.¹³ This mutation greatly reduces *KRAS*'s intrinsic GTPase activity, allowing for the accumulation of GTP-bound, active *KRAS*.¹⁴ Recently, the Shokat group identified molecules that covalently and selectively bind the mutated cysteine of *KRAS*^{G12C}.^{15–18} These compounds induce a novel, drug-like pocket within the *KRAS* switch II region.¹⁵ Optimization of the electrophiles responsible for conjugating the cysteine as well as the molecular interactions within the drug-induced pocket have led to the development of orally bioavailable *KRAS*^{G12C} inhibitors. *ARS-1620/ARS-3248*, *AMG510*, and *MRTX849*, developed by Wellspring, Amgen, and Mirati Therapeutics, respectively, have been shown to potentially inhibit *KRAS*^{G12C} activity *in vitro* and *in vivo*.^{19–22} In addition, *ARS-3248*, *AMG510*, and *MRTX849* have entered phase I clinical trials and have shown promising results.²³ However, despite this success, rapid adaptive resistance and MAPK signaling reactivation after inhibitor treatment have already been reported.^{24,25} Thus, the development of complementary therapeutic strategies could help realize the full potential of targeting *KRAS* mutants for cancer treatment.

Received: April 7, 2020

Published: July 8, 2020



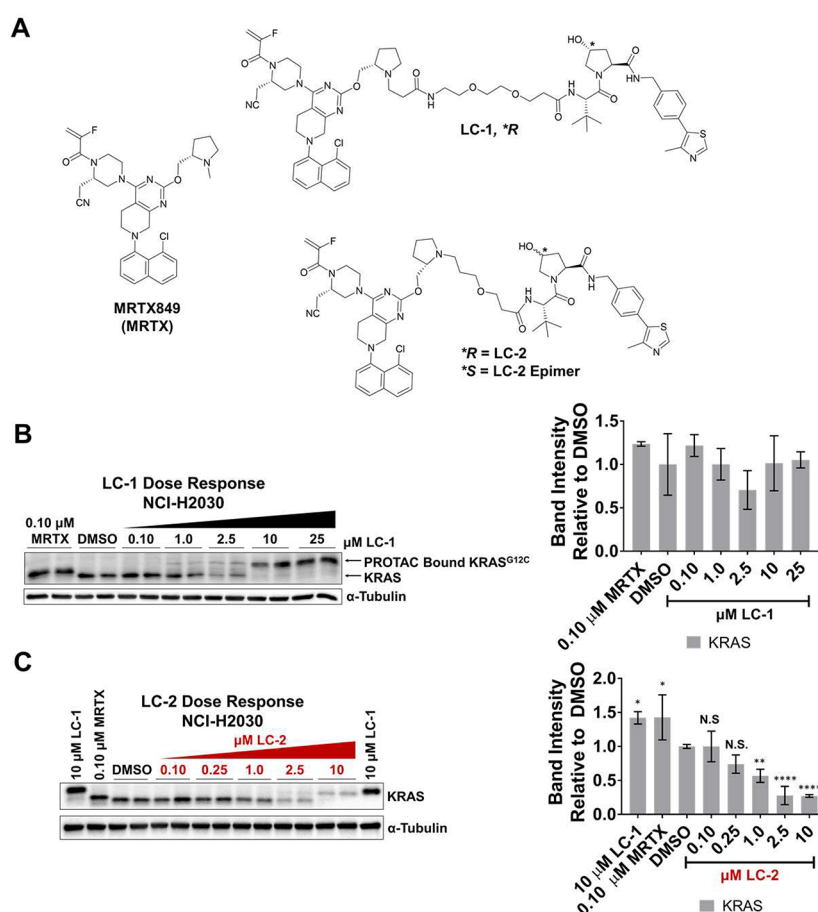


Figure 1. MRTX849-VHL PROTACs engage and degrade endogenous KRAS^{G12C} in NCI-H2030 cells. (A) Chemical structures of MRTX849, LC-1 (inactive PROTAC), LC-2 (active PROTAC), and LC-2 Epimer. (B) LC-1 engages KRAS^{G12C} in a dose-dependent manner. Quantitation on the right. (C) LC-2 degrades KRAS^{G12C} in a dose-dependent manner. Cells were treated for 24 h. Immunoblots show lysates from independent wells harvested side-by-side on the same day. Quantitation on the right. Quantified data represents mean \pm SD from two independent biological replicates. Not Significant (N.S.); * $p < 0.05$; ** $p < 0.01$; **** $p < 0.001$.

PROteolysis Targeting Chimeras (PROTACs) have emerged as a new and promising modality in drug discovery.^{26–29} These bifunctional molecules simultaneously engage a protein of interest (POI) and an E3 ligase, forming a ternary complex, enabling the E3 ligase to ubiquitinate the POI on proximal lysine residues.^{30,31} The ubiquitinated POI is subsequently recognized and degraded by the 26S proteasome. A major advantage of target degradation is the elimination of scaffolding roles that are not typically attenuated by traditional small-molecule inhibitors.^{32–36} PROTACs incorporating ARS-1620 and the cereblon E3 ligase ligand pomalidomide were recently published by the Gray group.^{37,38} These molecules engage KRAS^{G12C} and degrade an artificial GFP-KRAS^{G12C} fusion protein but were unable to degrade endogenous KRAS. Herein, we report the development of the first-in-class endogenous KRAS^{G12C} degrader, LC-2, which combines MRTX849 with a VHL E3 ligase ligand.³⁹ We observe rapid degradation through a *bona fide* PROTAC mechanism in both homozygous and heterozygous KRAS^{G12C}-expressing cells. Acute and sustained degradation of KRAS^{G12C} in multiple cancer cell lines renders LC-2 a valuable tool compound to interrogate KRAS biology and represents a significant step toward the development of PROTAC-based candidate therapeutics that function by inducing oncogenic KRAS degradation.

RESULTS

MRTX849-Based VHL-Recruiting PROTACs Engage and Degrade Endogenous KRAS^{G12C} in Homozygous and Heterozygous Mutant Cell Lines. In view of its promising Phase I clinical data and synthetic tractability, we chose MRTX849 (MRTX in figures; Figure 1A) as a starting point to design KRAS-targeting PROTACs. Docking of MRTX849 in the “switch II” pocket of KRAS^{G12C} reveals the pyrrolidine group to be solvent exposed. This observation was confirmed by a recently published crystal structure (PDB: 6UT0; SI Figure 1A).⁴⁰ To avoid introducing another stereocenter at the 2, 3, or 4 position of the pyrrolidine and further complicating our synthetic route, we decided to build linkers from the *N*-methyl moiety of the pyrrolidine. We saw our first evidence of KRAS engagement with LC-1 (Figure 1A,B). When NCI-H2030 cells were treated with increasing concentrations of LC-1 for 24 h, we observed a clear band shift at 1, 2.5, 10, and 25 μ M, indicating the presence of PROTAC-conjugated KRAS (Figure 1B). However, only a small, nonsignificant reduction in KRAS levels was observed. These data indicate that LC-1 can engage KRAS^{G12C} but does not efficiently degrade the protein. As a result, LC-1 was subsequently used as a positive control for KRAS engagement during our PROTAC screen.

One major liability of LC-1 is the presence of a hydrolyzable amide within the linker. To address this liability, the linkers of subsequent PROTACs were extended directly from the pyrrolidine ring nitrogen. We screened a small library of PROTACs with linker lengths several atoms shorter than LC-1 (SI Table 1). Our screen suggests that shorter linker lengths (~6 atoms) enable the most robust KRAS^{G12C} degradation for MRTX849-based, VHL recruiting PROTACs. From this screen, we identified LC-2 as the most potent KRAS^{G12C}-degrading PROTAC (Figure 1A,C). LC-2 induced maximal degradation of endogenous KRAS^{G12C} at concentrations as low as 2.5 μM with a D_{\max} of ~80% and a DC_{50} of 0.59 ± 0.20 μM in NCI-H2030 cells (Figure 1C). At 10 μM LC-2, a KRAS^{G12C} band running at the same molecular weight as LC-1-modified KRAS^{G12C} was observed. The emergence of an undegraded higher molecular weight band at 10 μM LC-2 suggests the start of a “hook-effect” at high LC-2 concentrations. The “hook-effect” is a hallmark of PROTACs, whereby at high drug concentrations, the formation of unproductive dimers with target or with E3 ligase outcompete formation of the ternary complex necessary for degradation.⁴¹

MRTX849 is known to be selective for mutant KRAS^{G12C} over other KRAS mutants.²¹ To explore the specificity of LC-2, KRAS degradation was examined in HCT 116 cells, which harbor a heterozygous KRAS^{G13D} mutation. No engagement or degradation of KRAS^{G13D} was observed in the presence of LC-2 up to 10 μM (SI Figure 1B). These data further suggest that LC-2 selectively engages and degrades mutant KRAS^{G12C} protein.

In addition, we tested LC-2 in 5 different KRAS^{G12C} cell lines and observed DC_{50} values between 0.25 and 0.76 μM as well as D_{\max} values ranging from ~75–90% (Table 1 and SI

Table 1. LC-2 Induces Degradation of Endogenous KRAS^{G12C} in Multiple KRAS Mutant Cancer Cell Lines: PROTAC Activity in a Panel of KRAS^{G12C} Cancer Cell Lines^a

cell line	KRAS ^{G12C} genotype	DC_{50} (μM)	D_{\max} (%)	MRTX sensitivity ²¹
NCI-H2030	+/+	0.59 ± 0.20	~80	+
MIA PaCa-2	+/+	0.32 ± 0.08	~75	++
SW1573	+/+	0.76 ± 0.30	~90	-
NCI-H23	+/-	0.25 ± 0.080	~90	N/A
NCI-H358	+/-	0.52 ± 0.30	~40	+++

^aCells were treated with LC-2 for 24 h and then total KRAS levels were determined by immunoblotting as described in the SI. Data are from two biological replicates. DC_{50} is the concentration at which 50% of the maximal degradation (D_{\max}) is reached.

Figure 2A–D). LC-2 can degrade mutant KRAS in both homozygous and heterozygous cell lines with varying sensitivities to MRTX849.²¹ Total KRAS levels, unbound plus PROTAC-bound KRAS^{G12C} for homozygotes and wild type plus PROTAC-bound KRAS for heterozygotes, were quantified for analysis. The observed DC_{50} values are ~2.5–7.5 fold larger than the reported IC_{50} of MRTX849 (~0.10 μM) in many of the cell lines tested.¹⁹ We suspect that this rightward shift in activity is primarily due to decreased permeability of the larger PROTAC molecule compared with the smaller parent inhibitor, a common occurrence in PROTAC development.^{27–29}

We observed >50% degradation in NCI-H23 cells, which are heterozygous. Theoretically, since these cells carry one wild type and one mutant KRAS^{G12C} allele, one would expect a maximum of 50% degradation if expression were equal, as we see for NCI-H358 cells (SI Figure 2A). However, in siRNA knockdown experiments using KRAS^{G12C} specific siRNA, nearly complete loss of KRAS is observed for NCI-H23 cells, which is consistent with the degradation we observe with LC-2.⁴² We observed slight differences in DC_{50} and D_{\max} values for the various homozygous cell lines tested. For example, LC-2 induces ~75% KRAS^{G12C} degradation in NCI-H2030 cells and MIA PaCa-2 cells; however, the DC_{50} values are 0.59 ± 0.20 and 0.32 ± 0.08 μM, respectively. This difference in activity could be caused by a number of factors including KRAS^{G12C} or VHL expression levels, differences in sensitivity to MRTX849, differences in permeability between cell lines, and/or differences in drug efflux pump activity. Cumulatively, these data show that MRTX849-based, VHL-recruiting PROTACs can engage and degrade KRAS^{G12C} in multiple cancer cell lines.

LC-2-Induced KRAS^{G12C} Degradation Occurs via a Bona Fide PROTAC Mechanism. The hydroxy proline moiety of the VHL ligand confers binding to the E3 ligase, while inversion of the absolute stereochemistry of the 4-hydroxy proline moiety abrogates VHL binding.³⁹ Therefore, we synthesized LC-2 Epimer (Figure 1A) as a physicochemically matched negative control molecule that is unable to recruit VHL. When NCI-H2030 cells were treated with 2.5 μM LC-2 Epimer for 4 h, only KRAS engagement was observed, whereas 2.5 μM LC-2 induced significant degradation (~65%; Figure 2A).

PROTACs target proteins for degradation via the proteasome by facilitating their ubiquitination, which is dependent on the formation of a ternary complex^{26,30,31} between the POI, PROTAC and the E3 ligase—in this case, VHL. Since excess VHL ligand inhibits ternary complex formation, we performed competition experiments in NCI-H2030 cells that were pretreated for 1 h with molar excess of VHL ligand before being treated with 2.5 μM LC-2. Competition of LC-2 with VHL ligand rescued KRAS^{G12C} levels (Figure 2A) by preventing PROTAC engagement with VHL. However, the higher-molecular-weight KRAS^{G12C} band observed upon LC-2 treatment demonstrates that the PROTAC was nevertheless still able to engage KRAS^{G12C}.

Neddylation of CUL2, a VHL adaptor protein, is necessary for proper assembly and function of the VHL E3 ligase complex.⁴³ To further investigate whether LC-2 induced degradation of KRAS^{G12C} occurs via a bona fide PROTAC mechanism, NCI-H2030 cells were treated with 1 μM of the neddylation inhibitor MLN4924 or 1 μM of the proteasome inhibitor epoxomicin, before being treated with 2.5 μM LC-2.^{44,45} Both inhibitors rescued KRAS^{G12C} levels suggesting KRAS^{G12C} degradation by LC-2 is both proteasome- and neddylation-dependent (Figure 2A).

KRAS is tethered to the plasma membrane, and mono-ubiquitination of KRAS^{G12C} can induce endocytosis and degradation of KRAS^{G12C} through the lysosomal pathway.⁴⁶ Therefore, we also tested whether bafilomycin A1 (BafA1), an inhibitor of lysosomal acidification, could rescue KRAS^{G12C} degradation.⁴⁷ Pretreatment of NCI-H23 cells with BafA1 was unable to rescue LC-2 induced KRAS^{G12C} degradation, whereas neddylation inhibition again rescued KRAS degradation (Figure 2B). Taken together these data show that LC-2-induced KRAS^{G12C} degradation is dependent on ternary

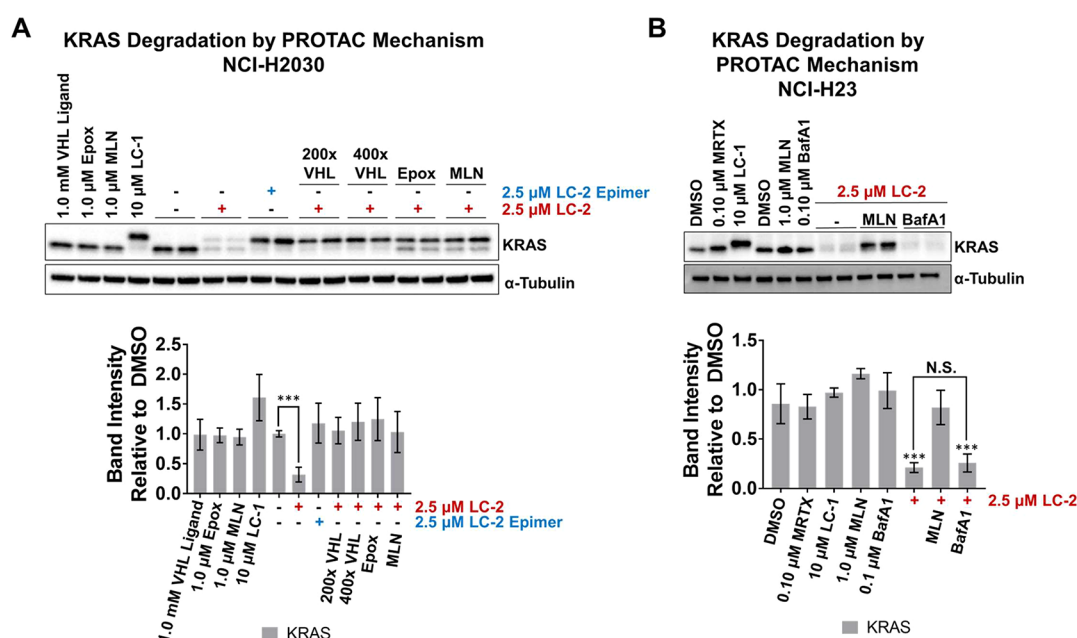


Figure 2. Degradation of endogenous KRAS^{G12C} is via a PROTAC mechanism. (A) LC-2 Epimer does not induce KRAS^{G12C} degradation at 2.5 μ M and LC-2 induced degradation is rescued by VHL ligand competition, proteasome inhibition with epoxomicin (Epox) and neddylation inhibition with MLN4924 (MLN) in NCI-H2030 cells. Immunoblots show lysates from independent wells harvested side-by-side on the same day. Quantitation is below. (B) Inhibition of neddylation, but not inhibition of lysosomal acidification, rescues LC-2 induced KRAS^{G12C} degradation in NCI-H23 cells. Quantitation is below. Quantified data represents mean \pm SD for two biological replicates. Not Significant (N.S.); *** $p < 0.005$

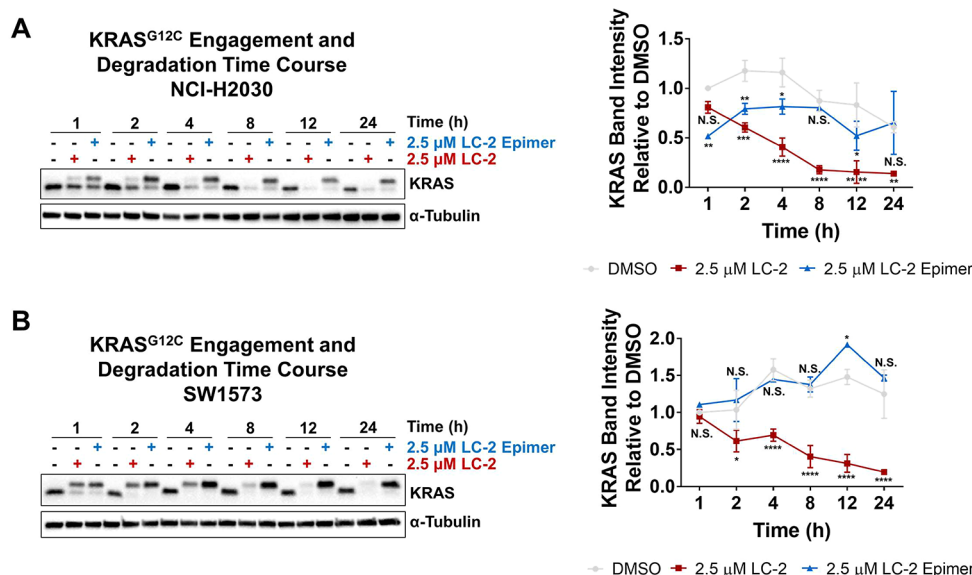


Figure 3. KRAS^{G12C} degradation is rapid, with maximal degradation induced as early as 4 h. (A) Time course in NCI-H2030 cells. LC-2 and LC-2 Epimer engage within 1 h with maximal degradation observed by 8 h and maintained up to 24 h. Quantitation on the right. (B) Time course in SW1573 cells. LC-2 and LC-2 epimer engage KRAS within 1 h and maximal degradation is observed at 12 h and maintained up to 24 h. Quantitation on the right. LC-2 Epimer is a quantification of the higher molecular weight, PROTAC Epimer modified band to monitor engagement of KRAS^{G12C} overtime rather than total KRAS levels. Quantified data represents mean \pm SD for two biological replicates. Not Significant (N.S.); * $p < 0.05$; ** $p < 0.01$; *** $p < 0.005$; **** $p < 0.001$.

complex formation with VHL and a functioning ubiquitin proteasome system, but not dependent on the lysosome.

LC-2 Induces Rapid and Sustained KRAS^{G12C} Degradation in Multiple Cancer Cell Lines. To explore PROTAC-induced KRAS^{G12C} degradation kinetics, time course experiments were performed in NCI-H2030 cells and SW1573 cells using 2.5 μ M LC-2 as the fixed concentration since it induced maximal degradation in all cell lines within 24

h (Figure 1A and SI Figure 2). To distinguish between rates of target engagement and degradation, LC-2 Epimer was used as a negative control to monitor KRAS^{G12C} engagement. Quantitation of engagement was achieved by comparing the intensity of just the LC-2 Epimer modified band to the intensity of unbound KRAS in DMSO-treated samples (see Materials and Methods). For NCI-H2030 cells, KRAS^{G12C} binding was seen as early as 1 h for both LC-2 and LC-2

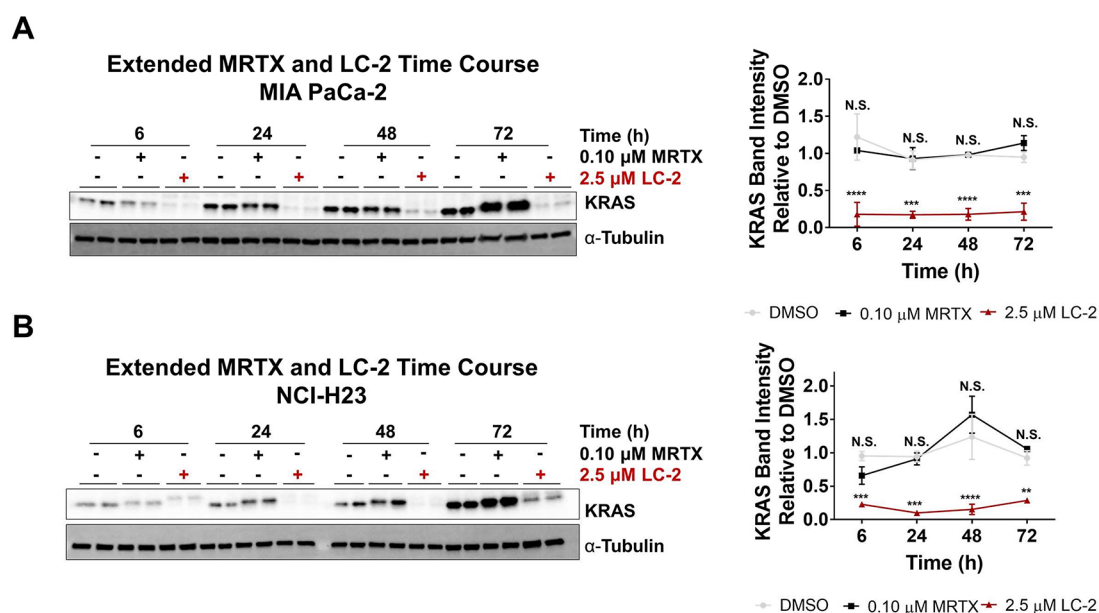


Figure 4. Degradation of endogenous KRAS^{G12C} is sustained over 72 h in multiple cancer cell lines. (A) 72 h time course in MIA PaCa-2 cells. Degradation occurs at 6 h and is maintained up to 72 h. Quantitation on the right. (B) 72 h time course in NCI-H23 cells. Degradation occurs within 6 h, reaches a maximum at 24 h, and begins to rebound by 72 h. Immunoblots show lysates from independent wells harvested side-by-side on the same day. Quantitation on the right. Quantified data represents mean \pm SD for two biological replicates. Not Significant (N.S.); ** $p < 0.01$; *** $p < 0.005$; **** $p < 0.001$.

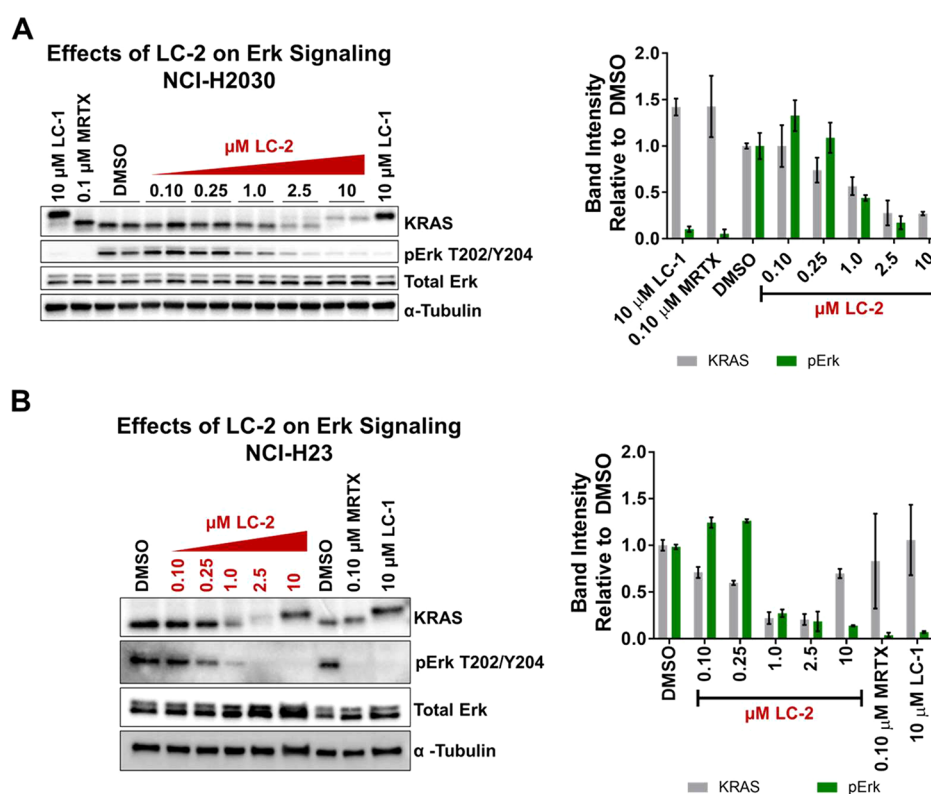


Figure 5. Degradation of endogenous KRAS^{G12C} modulates Erk signaling in homozygous and heterozygous KRAS^{G12C} cell lines. (A) Degradation of KRAS^{G12C} in homozygous NCI-H2030 cells attenuates pErk in a dose-dependent manner. Quantitation on the right. Immunoblots show lysates from independent wells harvested side-by-side on the same day. (B) Degradation of KRAS^{G12C} in heterozygous NCI-H23 cells decreases pErk in a dose-dependent manner. Quantitation on the right. For statistical analysis, see Supplemental Tables 2 and 3. Quantified data represents mean \pm SD for two biological replicates.

Epimer (Figure 3A). Maximal engagement and significant degradation occurred within 4 h. Maximum degradation was reached by 8 h in NCI-H2030 cells and persisted up to 24 h.

SW1573 cells showed faster kinetics with near maximal engagement at 1 h. However, the degradation rate was slower than NCI-H2030 cells as maximal degradation was not

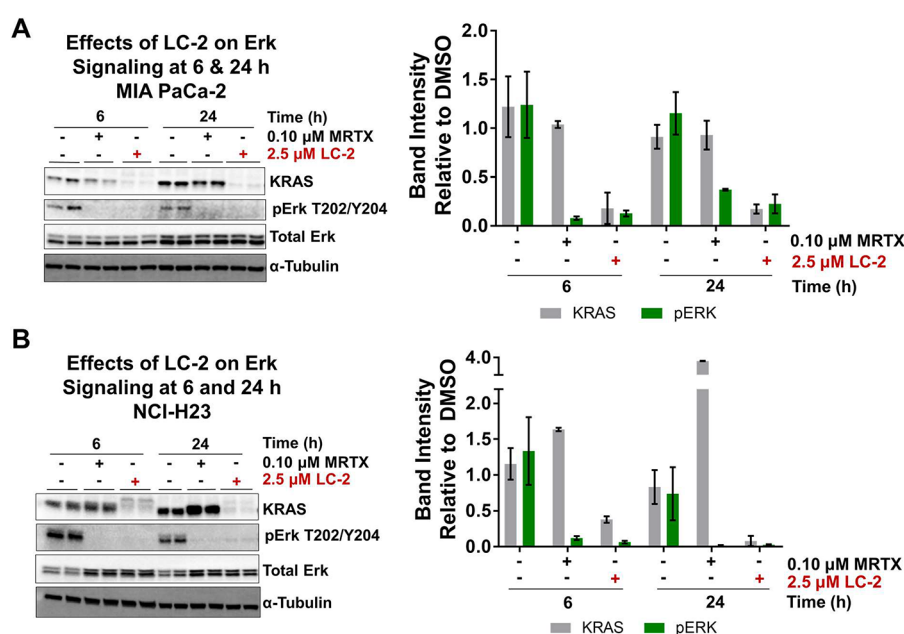


Figure 6. Effect of KRAS^{G12C} degradation and inhibition on Erk signaling over time. (A) Inhibition and degradation of KRAS^{G12C} decreases pErk signaling at 6 and 24 h in homozygous MIA PaCa-2 cells. Quantitation on the right. (B) Inhibition and degradation of KRAS^{G12C} decreases pErk signaling at 6 and 24 h in heterozygous NCI-H23. Immunoblots show lysates from independent wells harvested side-by-side on the same day. Quantitation on the right. For statistical analysis, see Supplemental Tables 4 and 5. Quantified data represents mean \pm SD for two biological replicates.

observed until 12 h (Figure 3B). Interestingly, LC-2 Epimer engaged KRAS^{G12C} faster than LC-2 in both cell lines. Differential engagement could arise if LC-2 first forms binary complexes with VHL in the cytosol, decreasing the effective concentration of LC-2 at the membrane available for conjugation with KRAS^{G12C}.

During our PROTAC screen, we observed that 0.10 μ M of MRTX849 and 10 μ M of LC-1 increased KRAS protein levels (Figure 1C). Our data is consistent with previous observations that treatment of cells with another KRAS^{G12C} inhibitor, ARS1620, leads to increased KRAS expression over time.^{19,21} Therefore, we explored how longer treatments with LC-2 would affect KRAS^{G12C} levels. MIA PaCa-2, NCI-H23, and SW1573 cells were treated with 2.5 μ M of LC-2 for 6, 24, 48, and 72 h. In all three cell lines, maximal KRAS degradation occurred within 24 h and was sustained up to 72 h (Figure 4A,B and SI Figure 3). LC-2 Epimer fully engaged KRAS^{G12C} in SW1573 cells, but did not decrease protein levels, as expected (SI Figure 3). In NCI-H23 cells, KRAS^{G12C} began to rebound at 72 h. The lack of KRAS^{G12C} protein level rebound in MIA PaCa-2 and SW1573 cells suggests that a sufficient excess of LC-2 is present in these cell lines to maintain maximal degradation despite resynthesis of KRAS^{G12C}. Taken together these data show that LC-2 is capable of inducing rapid and sustained KRAS^{G12C} degradation in both homozygous and heterozygous cell lines. The ability to overcome increased KRAS^{G12C} expression suggests that degradation could be more beneficial than inhibition for prolonged attenuation of downstream signaling as has been observed previously with BRD4 degraders.⁴⁸

LC-2-Induced KRAS^{G12C} Degradation Modulates Erk Signaling in Homozygous and Heterozygous KRAS Mutant Cell Lines. The ability of LC-2 to modulate Erk signaling was investigated in NCI-H2030 and NCI-H23 cells during a 24 h dose response. A dose-dependent decrease in

pErk signaling was observed in both NCI-H2030 and NCI-H23 cells (Figure 5).

Signaling kinetics were monitored during a 24 h time course in MIA PaCa-2, NCI-H23, and SW1573 cells treated with 2.5 μ M LC-2. Modulation of Erk signaling by both MRTX849 and LC-2 occurs within 6 h in MIA PaCa-2 and NCI-H23 cells (Figure 6A,B). pErk was suppressed by both compounds at 6 and 24 h in each cell line. In SW1573 cells, phosphorylated Erk was inhibited by 2.5 μ M LC-2 between 1 and 4 h; however, pErk levels rebounded between 8 and 24 h (SI Figure 4). Nonetheless, pErk levels were still significantly lower in LC-2-treated cells than DMSO-treated cells at 24 h. Total Erk was increased in LC-2-treated cells compared with DMSO at all time points indicating the initiation of a positive feedback loop upon KRAS^{G12C} degradation and pErk inhibition (SI Figure 4). Taken together, these data show that LC-2-induced KRAS^{G12C} degradation is capable of modulating downstream signaling and that differences in signaling between inhibition and degradation are cell line dependent.

DISCUSSION

To our knowledge, this study is the first report of PROTAC-induced endogenous KRAS^{G12C} degradation in cancer cells. Our PROTAC, LC-2, couples the covalent KRAS^{G12C} inhibitor MRTX849 to the VHL ligand developed in our laboratory.^{21,39} VHL recruitment to KRAS^{G12C} induces endogenous KRAS ubiquitination and degradation with DC₅₀ values ranging from 0.25 to 0.76 μ M. We observe rapid engagement, sustained KRAS degradation, and attenuated pErk signaling for up to 72 h in several KRAS^{G12C} mutant cell lines. This tool compound will facilitate further exploration of how KRAS degradation influences downstream signaling and the viability of KRAS^{G12C} mutant cancer cells with more precise temporal control than nucleic acid-based knockdown methods.

This work is not the first attempt at degrading KRAS^{G12C}. Recently, Zeng et al. were unsuccessful in degrading endogenous KRAS^{G12C} with 20 μ M of XY-4–88 over 24 h.³⁸ That PROTAC was based on ARS1620 and used pomalidomide to recruit cereblon, whereas our active PROTAC, LC-2, is MRTX849-based and recruits VHL. It has been our observation that differences in either constituent ligand of a PROTAC can significantly impact the efficacy and selectivity of target engagement.^{31,49} Further studies will focus on understanding the importance of the KRAS^{G12C} ligand, the recruited E3 ligase, or the combination of these two factors in imparting LC-2's activity. Conducting ternary complex assays by SPR and/or monitoring the ability of these compounds to induce ubiquitination by using tandem ubiquitin binding entity (TUBE) pull-downs followed by immunoblotting could address these questions.⁵⁰

With the availability of several new covalent inhibitors, kinome rewiring in response to KRAS^{G12C} inhibition has been an active research area. It has been found that signaling attenuated by MRTX849, AMG510, and ARS1620 returns to or exceeds basal levels between 24 and 72 h.^{21,24,25} This has been linked to the increased activity of several tyrosine kinases. To combat this acquired resistance, pan-RTK, FGFR, or SHP2 inhibitors in combination with KRAS^{G12C} inhibition have been successfully used to reduce the recovery of signaling.²⁴ These cotreatment regimens have also been shown to be more antiproliferative *in vitro* and *in vivo* compared to RTK inhibition or KRAS^{G12C} inhibition alone.^{24,51} It will be interesting to determine whether LC-2 induced degradation alone can overcome Erk signaling reactivation and/or if combination of KRAS degradation with RTK inhibition could further enhance antiproliferative effects. In addition to the rewiring of sensitive cells, there are known cell lines, such as SW1573 (used in this work) and NCI-H1792, that are inherently resistant to the antiproliferative effects of KRAS^{G12C} inhibition. Recently, it was shown that siRNA mediated knockdown in these cells, but not KRAS^{G12C} inhibition, resulted in ~50% decreased cell viability.⁵¹ Therefore, it will be interesting to determine if KRAS^{G12C}-induced degradation of KRAS^{G12C} by LC-2 is also similarly antiproliferative in these cell lines.

The major caveat of LC-2 is that the covalent nature of the PROTAC may limit its potency as it cannot participate in catalytic rounds of degradation. This may negatively impact the maximal inhibition of KRAS signaling and the effectiveness of LC-2 in an *in vivo* setting.³⁰ Additionally, this limits LC-2's effect on cell viability. MRTX849 was more antiproliferative in homozygous NCI-H2030 and heterozygous NCI-H23 cells than LC-2 (SI Figure 5). More potent, catalytic PROTACs will be needed to better compare the effects of KRAS degradation vs inhibition. Therefore, efforts to develop reversible PROTACs to target KRAS mutants are warranted. LC-2 provides a great starting point for the development of more potent KRAS degraders.

The ability to target KRAS with covalent inhibitors was itself a milestone in drug discovery. It showed that KRAS, an "undruggable" protein, could be directly inhibited by a small molecule. Similarly, the results presented here demonstrate for the first time that endogenous KRAS^{G12C} can be degraded as long as a suitable ligand is identified. While ligand development for other KRAS mutants continues, LC-2 can serve as a tool compound to investigate biology in the context of rapid KRAS^{G12C} degradation. Despite its limitations, the discovery of

LC-2 opens new opportunities for targeting KRAS mutants in cancer therapy.

■ ASSOCIATED CONTENT

Supporting Information

The Supporting Information is available free of charge at <https://pubs.acs.org/doi/10.1021/acscentsci.0c00411>.

Crystal structure of MRTX849 bound to KRASG12C, LC-2 dose response in HCT116, LC-2 dose responses in homo/heterozygous cell KRASG12C cell lines, 72 h LC-2 and LC-2 Epimer time course in SW1573 cells, effect of LC-2 on pErk and total Erk levels in SW1573 cells over 24 h, and cell viability experiment (Supplemental Figures 1–5); Structures and activity of all PROTACs test and statistical analysis (Supplemental Tables 1–6); materials and methods; and chemical synthesis (PDF)

■ AUTHOR INFORMATION

Corresponding Author

Craig M. Crews – Department of Pharmacology, Department of Molecular, Cellular, and Developmental Biology, and Department of Chemistry, Yale University, New Haven, Connecticut 06511, United States; orcid.org/0000-0002-8456-2005; Email: craig.crews@yale.edu

Authors

Michael J. Bond – Department of Pharmacology, Yale University, New Haven, Connecticut 06511, United States

Ling Chu – Department of Molecular, Cellular, and Developmental Biology, Yale University, New Haven, Connecticut 06511, United States

Dhanusha A. Nalawansa – Department of Molecular, Cellular, and Developmental Biology, Yale University, New Haven, Connecticut 06511, United States

Ke Li – Department of Molecular, Cellular, and Developmental Biology, Yale University, New Haven, Connecticut 06511, United States

Complete contact information is available at:

<https://pubs.acs.org/doi/10.1021/acscentsci.0c00411>

Author Contributions

[¶](M.J.B., L.C.) These authors contributed equally to this work

Notes

The authors declare the following competing financial interest(s): C.M.C. is founder, shareholder, and consultant to Arvinas, Inc., which supports research in his laboratory.

■ ACKNOWLEDGMENTS

We would like to thank Dr. Saul Jaime-Figueroa for assisting with the MRTX849 docking and Dr. John Hines for his insight, comments and critiques in the preparation of this manuscript. We would also like to thank Dr. Kanak Raina for his helpful comments in the project. C.M.C. is funded by the NIH (R35CA197589) and is supported by an American Cancer Research Professorship. M.J.B. acknowledges support from the NIH (F31CA232477 and 5T32GM067543).

■ REFERENCES

(1) Prior, I. A.; Lewis, P. D.; Mattos, C. A comprehensive survey of Ras mutations in cancer. *Cancer Res.* **2012**, *72* (10), 2457–2467.

- (2) Land, H.; Parada, L. F.; Weinberg, R. A. Tumorigenic conversion of primary embryo fibroblasts requires at least two cooperating oncogenes. *Nature* **1983**, *304* (5927), 596–602.
- (3) Newbold, R. F.; Overell, R. W. Fibroblast Immortality Is a Prerequisite for Transformation by E₁C-Ha-Ras Oncogene. *Nature* **1983**, *304* (5927), 648–651.
- (4) Milburn, M. V.; Tong, L.; Devos, A. M.; Brunger, A.; Yamaizumi, Z.; Nishimura, S.; Kim, S. H. Molecular Switch for Signal Transduction - Structural Differences between Active and Inactive Forms of Protooncogenic Ras Proteins. *Science* **1990**, *247* (4945), 939–945.
- (5) Simanshu, D. K.; Nissley, D. V.; McCormick, F. RAS Proteins and Their Regulators in Human Disease. *Cell* **2017**, *170* (1), 17–33.
- (6) Ito, Y.; Yamasaki, K.; Iwahara, J.; Terada, T.; Kamiya, A.; Shirouzu, M.; Muto, Y.; Kawai, G.; Yokoyama, S.; Laue, E. D.; et al. Regional polyserism in the GTP-bound form of the human c-Ha-Ras protein. *Biochemistry* **1997**, *36* (30), 9109–9119.
- (7) Bar-Sagi, D. The Sos (Son of sevenless) protein. *Trends Endocrinol. Metab.* **1994**, *5* (4), 165–169.
- (8) Pierre, S.; Bats, A. S.; Coumoul, X. Understanding SOS (Son of Sevenless). *Biochem. Pharmacol.* **2011**, *82* (9), 1049–1056.
- (9) Harrell Stewart, D. R.; Clark, G. J. Pumping the brakes on RAS - negative regulators and death effectors of RAS. *J. Cell Sci.* **2020**, *133* (3), jcs238865.
- (10) Boriack-Sjodin, P. A.; Margarit, S. M.; Bar-Sagi, D.; Kuriyan, J. The structural basis of the activation of Ras by Sos. *Nature* **1998**, *394* (6691), 337–343.
- (11) Scheffzek, K.; Ahmadian, M. R.; Kabsch, W.; Wiesmuller, L.; Lautwein, A.; Schmitz, F.; Wittinghofer, A. The Ras-RasGAP complex: structural basis for GTPase activation and its loss in oncogenic Ras mutants. *Science* **1997**, *277* (5324), 333–338.
- (12) Spencer-Smith, R.; O'Bryan, J. P. Direct inhibition of RAS: Quest for the Holy Grail? *Semin. Cancer Biol.* **2019**, *54*, 138–148.
- (13) Campbell, J. D.; Alexandrov, A.; Kim, J.; Wala, J.; Berger, A. H.; Pedamallu, C. S.; Shukla, S. A.; Guo, G.; Brooks, A. N.; Murray, B. A.; et al. Distinct patterns of somatic genome alterations in lung adenocarcinomas and squamous cell carcinomas. *Nat. Genet.* **2016**, *48* (6), 607–616.
- (14) Lu, S.; Banerjee, A.; Jang, H.; Zhang, J.; Gaponenko, V.; Nussinov, R. GTP Binding and Oncogenic Mutations May Attenuate Hypervariable Region (HVR)-Catalytic Domain Interactions in Small GTPase K-Ras4B, Exposing the Effector Binding Site. *J. Biol. Chem.* **2015**, *290* (48), 28887–28900.
- (15) Ostrem, J. M.; Peters, U.; Sos, M. L.; Wells, J. A.; Shokat, K. M. K-Ras(G12C) inhibitors allosterically control GTP affinity and effector interactions. *Nature* **2013**, *503* (7477), 548–551.
- (16) Rudolph, J.; Stokoe, D. Selective inhibition of mutant Ras protein through covalent binding. *Angew. Chem., Int. Ed.* **2014**, *53* (15), 3777–3779.
- (17) Ostrem, J. M.; Shokat, K. M. Direct small-molecule inhibitors of KRAS: from structural insights to mechanism-based design. *Nat. Rev. Drug Discovery* **2016**, *15* (11), 771–785.
- (18) Nnadi, C. I.; Jenkins, M. L.; Gentile, D. R.; Bateman, L. A.; Zaidman, D.; Balius, T. E.; Nomura, D. K.; Burke, J. E.; Shokat, K. M.; London, N. Novel K-Ras G12C Switch-II Covalent Binders Destabilize Ras and Accelerate Nucleotide Exchange. *J. Chem. Inf. Model.* **2018**, *58* (2), 464–471.
- (19) Janes, M. R.; Zhang, J.; Li, L. S.; Hansen, R.; Peters, U.; Guo, X.; Chen, Y.; Babbar, A.; Firdaus, S. J.; Darjanian, L.; et al. Targeting KRAS Mutant Cancers with a Covalent G12C-Specific Inhibitor. *Cell* **2018**, *172* (3), 578.
- (20) Canon, J.; Rex, K.; Saiki, A. Y.; Mohr, C.; Cooke, K.; Bagal, D.; Gaida, K.; Holt, T.; Knutson, C. G.; Koppada, N.; et al. The clinical KRAS(G12C) inhibitor AMG 510 drives anti-tumour immunity. *Nature* **2019**, *575* (7781), 217–223.
- (21) Hallin, J.; Engstrom, L. D.; Hargis, L.; Calinisan, A.; Aranda, R.; Briere, D. M.; Sudhakar, N.; Bowcut, V.; Baer, B. R.; Ballard, J. A.; et al. The KRAS(G12C) Inhibitor MRTX849 Provides Insight toward Therapeutic Susceptibility of KRAS-Mutant Cancers in Mouse Models and Patients. *Cancer Discovery* **2020**, *10* (1), 54–71.
- (22) Race for undruggable KRAS speeds up. *Nat. Biotechnol.* **2019**, *37* (11), 1247, DOI: 10.1038/s41587-019-0312-y.
- (23) Seton-Rogers, S. KRAS-G12C in the crosshairs. *Nat. Rev. Cancer* **2020**, *20* (1), 3.
- (24) Ryan, M. B.; Fece de la Cruz, F.; Phat, S.; Myers, D. T.; Wong, E.; Shahzade, H. A.; Hong, C. B.; Corcoran, R. B. Vertical Pathway Inhibition Overcomes Adaptive Feedback Resistance to KRAS-(G12C) Inhibition. *Clin. Cancer Res.* **2020**, *26*, 1633.
- (25) Xue, J. Y.; Zhao, Y.; Aronowitz, J.; Mai, T. T.; Vides, A.; Qeriqi, B.; Kim, D.; Li, C.; de Stanchina, E.; Mazutis, L.; et al. Rapid non-uniform adaptation to conformation-specific KRAS(G12C) inhibition. *Nature* **2020**, *577* (7790), 421–425.
- (26) Sakamoto, K. M.; Kim, K. B.; Kumagai, A.; Mercurio, F.; Crews, C. M.; Deshaies, R. J. Protacs: Chimeric molecules that target proteins to the Skp1-Cullin-F box complex for ubiquitination and degradation. *Proc. Natl. Acad. Sci. U. S. A.* **2001**, *98* (15), 8554–8559.
- (27) Burslem, G. M.; Crews, C. M. Proteolysis-Targeting Chimeras as Therapeutics and Tools for Biological Discovery. *Cell* **2020**, *181*, 102.
- (28) Paiva, S. L.; Crews, C. M. Targeted protein degradation: elements of PROTAC design. *Curr. Opin. Chem. Biol.* **2019**, *50*, 111–119.
- (29) Pettersson, M.; Crews, C. M. Proteolysis TArgeting Chimeras (PROTACs) - Past, present and future. *Drug Discovery Today: Technol.* **2019**, *31*, 15–27.
- (30) Bondeson, D. P.; Mares, A.; Smith, I. E. D.; Ko, E.; Campos, S.; Miah, A. H.; Mulholland, K. E.; Routly, N.; Buckley, D. L.; Gustafson, J. L.; et al. Catalytic in vivo protein knockdown by small-molecule PROTACs. *Nat. Chem. Biol.* **2015**, *11* (8), 611–U120.
- (31) Bondeson, D. P.; Smith, B. E.; Burslem, G. M.; Buhimschi, A. D.; Hines, J.; Jaime-Figueroa, S.; Wang, J.; Hamman, B. D.; Ishchenko, A.; Crews, C. M. Lessons in PROTAC Design from Selective Degradation with a Promiscuous Warhead. *Cell Chemical Biology* **2018**, *25* (1), 78.
- (32) Burslem, G. M.; Smith, B. E.; Lai, A. C.; Jaime-Figueroa, S.; McQuaid, D. C.; Bondeson, D. P.; Toure, M.; Dong, H. Q.; Qian, Y. M.; Wang, J.; et al. The Advantages of Targeted Protein Degradation Over Inhibition: An RTK Case Study. *Cell Chemical Biology* **2018**, *25* (1), 67.
- (33) Salami, J.; Alabi, S.; Willard, R. R.; Vitale, N. J.; Wang, J.; Dong, H. Q.; Jin, M. Z.; McDonnell, D. P.; Crew, A. P.; Neklesa, T. K. Androgen receptor degradation by the proteolysis-targeting chimera ARCC-4 outperforms enzalutamide in cellular models of prostate cancer drug resistance. *Commun. Biol.* **2018**, *1*, 100.
- (34) Cromm, P. M.; Samarasinghe, K. T. G.; Hines, J.; Crews, C. M. Addressing Kinase-Independent Functions of Fak via PROTAC-Mediated Degradation. *J. Am. Chem. Soc.* **2018**, *140* (49), 17019–17026.
- (35) Burslem, G. M.; Song, J. Y.; Chen, X.; Hines, J.; Crews, C. M. Enhancing Antiproliferative Activity and Selectivity of a FLT-3 Inhibitor by Proteolysis Targeting Chimera Conversion. *J. Am. Chem. Soc.* **2018**, *140* (48), 16428–16432.
- (36) Burslem, G. M.; Schultz, A. R.; Bondeson, D. P.; Eide, C. A.; Stevens, S. L. S.; Druker, B. J.; Crews, C. M. Targeting BCR-ABL1 in Chronic Myeloid Leukemia by PROTAC-Mediated Targeted Protein Degradation. *Cancer Res.* **2019**, *79* (18), 4744–4753.
- (37) Ito, T.; Ando, H.; Suzuki, T.; Ogura, T.; Hotta, K.; Imamura, Y.; Yamaguchi, Y.; Handa, H. Identification of a Primary Target of Thalidomide Teratogenicity. *Science* **2010**, *327* (5971), 1345–1350.
- (38) Zeng, M.; Xiong, Y.; Safaei, N.; Nowak, R. P.; Donovan, K. A.; Yuan, C. J.; Nabet, B.; Gero, T. W.; Feru, F.; Li, L.; et al. Exploring Targeted Degradation Strategy for Oncogenic KRAS(G12C). *Cell Chem. Biol.* **2020**, *27* (1), 19.
- (39) Buckley, D. L.; Van Molle, I.; Gareiss, P. C.; Tae, H. S.; Michel, J.; Noblin, D. J.; Jorgensen, W. L.; Ciulli, A.; Crews, C. M. Targeting the von Hippel-Lindau E3 Ubiquitin Ligase Using Small Molecules

To Disrupt the VHL/HIF-1 alpha Interaction. *J. Am. Chem. Soc.* **2012**, *134* (10), 4465–4468.

(40) Fell, J. B.; Fischer, J. P.; Baer, B. R.; Blake, J. F.; Bouhana, K.; Briere, D. M.; Brown, K. D.; Burgess, L. E.; Burns, A. C.; Burkard, M. Ret al. Identification of the Clinical Development Candidate MRTX849, a Covalent KRAS(G12C) Inhibitor for the Treatment of Cancer. *J. Med. Chem.* **2020**, DOI: DOI: 10.1021/acs.jmedchem.9b02052.

(41) Buckley, D. L.; Raina, K.; Darricarrere, N.; Hines, J.; Gustafson, J. L.; Smith, I. E.; Miah, A. H.; Harling, J. D.; Crews, C. M. HaloPROTACS: Use of Small Molecule PROTACs to Induce Degradation of HaloTag Fusion Proteins. *ACS Chem. Biol.* **2015**, *10* (8), 1831–1837.

(42) Sunaga, N.; Shames, D. S.; Girard, L.; Peyton, M.; Larsen, J. E.; Imai, H.; Soh, J.; Sato, M.; Yanagitani, N.; Kaira, K.; et al. Knockdown of oncogenic KRAS in non-small cell lung cancers suppresses tumor growth and sensitizes tumor cells to targeted therapy. *Mol. Cancer Ther.* **2011**, *10* (2), 336–346.

(43) Merlet, J.; Burger, J.; Gomes, J. E.; Pintard, L. Regulation of cullin-RING E3 ubiquitin-ligases by neddylation and dimerization. *Cell. Mol. Life Sci.* **2009**, *66* (11–12), 1924–1938.

(44) Meng, L.; Mohan, R.; Kwok, B. H.; Eloffsson, M.; Sin, N.; Crews, C. M. Epoxomicin, a potent and selective proteasome inhibitor, exhibits in vivo antiinflammatory activity. *Proc. Natl. Acad. Sci. U. S. A.* **1999**, *96* (18), 10403–10408.

(45) Soucy, T. A.; Smith, P. G.; Milhollen, M. A.; Berger, A. J.; Gavin, J. M.; Adhikari, S.; Brownell, J. E.; Burke, K. E.; Cardin, D. P.; Critchley, S.; et al. An inhibitor of NEDD8-activating enzyme as a new approach to treat cancer. *Nature* **2009**, *458* (7239), 732–U767.

(46) Lu, A.; Tebar, F.; Alvarez-Moya, B.; Lopez-Alcala, C.; Calvo, M.; Enrich, C.; Agell, N.; Nakamura, T.; Matsuda, M.; Bachs, O. A clathrin-dependent pathway leads to KRas signaling on late endosomes en route to lysosomes. *J. Cell Biol.* **2009**, *184* (6), 863–879.

(47) Oda, K.; Nishimura, Y.; Ikehara, Y.; Kato, K. Bafilomycin-A1 Inhibits the Targeting of Lysosomal Acid-Hydrolases in Cultured-Hepatocytes. *Biochem. Biophys. Res. Commun.* **1991**, *178* (1), 369–377.

(48) Lu, J.; Qian, Y.; Altieri, M.; Dong, H.; Wang, J.; Raina, K.; Hines, J.; Winkler, J. D.; Crew, A. P.; Coleman, K.; et al. Hijacking the E3 Ubiquitin Ligase Cereblon to Efficiently Target BRD4. *Chem. Biol.* **2015**, *22* (6), 755–763.

(49) Lai, A. C.; Toure, M.; Hellerschmied, D.; Salami, J.; Jaime-Figueroa, S.; Ko, E.; Hines, J.; Crews, C. M. Modular PROTAC Design for the Degradation of Oncogenic BCR-ABL. *Angew. Chem., Int. Ed.* **2016**, *55* (2), 807–810.

(50) Hjerpe, R.; Aillet, F.; Lopitz-Otsoa, F.; Lang, V.; England, P.; Rodriguez, M. S. Efficient protection and isolation of ubiquitylated proteins using tandem ubiquitin-binding entities. *EMBO Rep.* **2009**, *10* (11), 1250–1258.

(51) Misale, S.; Fatherree, J. P.; Cortez, E.; Li, C.; Bilton, S.; Timonina, D.; Myers, D. T.; Lee, D.; Gomez-Caraballo, M.; Greenberg, M.; et al. KRAS G12C NSCLC Models Are Sensitive to Direct Targeting of KRAS in Combination with PI3K Inhibition. *Clin. Cancer Res.* **2019**, *25* (2), 796–807.